



HAL
open science

Evidence for higher-than-average air temperatures after the 8.2 ka event provided by a Central European $\delta^{18}\text{O}$ record

Nils Andersen, Stefan Lauterbach, Helmut Erlenkeuser, Dan Danielopol, Tadeusz Namiotko, Matthias Hüls, Soumaya Belmecheri, Peter Dulski, Carla Nantke, Hanno Meyer, et al.

► To cite this version:

Nils Andersen, Stefan Lauterbach, Helmut Erlenkeuser, Dan Danielopol, Tadeusz Namiotko, et al.. Evidence for higher-than-average air temperatures after the 8.2 ka event provided by a Central European $\delta^{18}\text{O}$ record. *Quaternary Science Reviews*, 2017, 172, pp.96-108. 10.1016/j.quascirev.2017.08.001 . hal-02461927

HAL Id: hal-02461927

<https://hal.science/hal-02461927>

Submitted on 18 Nov 2020

HAL is a multi-disciplinary open access archive for the deposit and dissemination of scientific research documents, whether they are published or not. The documents may come from teaching and research institutions in France or abroad, or from public or private research centers.

L'archive ouverte pluridisciplinaire **HAL**, est destinée au dépôt et à la diffusion de documents scientifiques de niveau recherche, publiés ou non, émanant des établissements d'enseignement et de recherche français ou étrangers, des laboratoires publics ou privés.



Evidence for higher-than-average air temperatures after the 8.2 ka event provided by a Central European $\delta^{18}\text{O}$ record



Nils Andersen ^a, Stefan Lauterbach ^{b, c, *}, Helmut Erlenkeuser ^a, Dan L. Danielopol ^{d, 3}, Tadeusz Namiotko ^e, Matthias Hüls ^a, Soumaya Belmecheri ^{f, 1}, Peter Dulski ^b, Carla Nantke ^{b, 2}, Hanno Meyer ^g, Bernhard Chaplign ^g, Ulrich von Grafenstein ^f, Achim Brauer ^b

^a University of Kiel, Leibniz Laboratory for Radiometric Dating and Stable Isotope Research, 24118 Kiel, Germany

^b GFZ German Research Centre for Geosciences, Section 5.2 – Climate Dynamics and Landscape Evolution, 14473 Potsdam, Germany

^c University of Innsbruck, Institute of Geology, 6020 Innsbruck, Austria

^d University of Graz, Institute of Earth Sciences (Geology & Palaeontology), 8010 Graz, Austria

^e University of Gdańsk, Faculty of Biology, Department of Genetics, Laboratory of Limnology, 80-308 Gdańsk, Poland

^f Laboratoire des Sciences du Climat et de l'Environnement, UMR 8212, CEA-CNRS-UVSQ, 91191 Gif-sur-Yvette, France

^g Alfred Wegener Institute, Helmholtz Centre for Polar and Marine Research, Periglacial Research Section, 14473 Potsdam, Germany

ARTICLE INFO

Article history:

Received 21 February 2017

Received in revised form

26 July 2017

Accepted 1 August 2017

Keywords:

Holocene

Palaeoclimatology

Europe

Stable isotopes

8.2 ka event

Lake sediments

ABSTRACT

The so-called 8.2 ka event represents one of the most prominent cold climate anomalies during the Holocene warm period. Accordingly, several studies have addressed its trigger mechanisms, absolute dating and regional characteristics so far. However, knowledge about subsequent climate recovery is still limited although this might be essential for the understanding of rapid climatic changes. Here we present a new sub-decadally resolved and precisely dated oxygen isotope ($\delta^{18}\text{O}$) record for the interval between 7.7 and 8.7 ka BP (10^3 calendar years before AD 1950), derived from the calcareous valves of benthic ostracods preserved in the varved lake sediments of pre-Alpine Mondsee (Austria). Besides a clear reflection of the 8.2 ka event, showing a good agreement in timing, duration and magnitude with other regional stable isotope records, the high-resolution Mondsee lake sediment record provides evidence for a 75-year-long interval of higher-than-average $\delta^{18}\text{O}$ values directly after the 8.2 ka event, possibly reflecting increased air temperatures in Central Europe. This observation is consistent with evidence from other proxy records in the North Atlantic realm, thus most probably reflecting a hemispheric-scale climate signal rather than a local phenomenon. As a possible trigger we suggest an enhanced resumption of the Atlantic meridional overturning circulation (AMOC), supporting assumptions from climate model simulations.

© 2017 Elsevier Ltd. All rights reserved.

1. Introduction

The Holocene warm period has been punctuated by several

short-term climate perturbations (Mayewski et al., 2004) with that around 8.2 ka BP (10^3 calendar years before AD 1950) being a particularly prominent one (Alley and Ágústssdóttir, 2005; Alley et al., 1997; Rohling and Pälike, 2005). This cold episode, commonly termed 8.2 ka event, is generally considered as having been triggered by the catastrophic drainage of the Laurentide proglacial lakes Agassiz and Ojibway after the collapse of the Hudson Bay ice dome (Barber et al., 1999; Teller et al., 2002; von Grafenstein et al., 1998). The associated sudden input of a large amount of freshwater into the North Atlantic caused a salinity/density reduction of the ocean surface waters and consequently a transient slowdown of the Atlantic meridional overturning circulation (AMOC; Ellison et al., 2006; Kleiven et al., 2008). This

* Corresponding author. University of Innsbruck, Institute of Geology, 6020 Innsbruck, Austria.

E-mail address: stefan.lauterbach@uibk.ac.at (S. Lauterbach).

¹ Present address: University of Arizona, Laboratory of Tree-Ring Research, AZ 85721 Tucson, USA.

² Present address: Lund University, Department of Geology, 223 62 Lund, Sweden.

³ Former address: Austrian Academy of Sciences, Institute for Limnology, 5310 Mondsee, Austria.

resulted in reduced northward heat transport, leading to a pronounced cooling in the North Atlantic realm (Alley and Ágústsdóttir, 2005; Morrill and Jacobsen, 2005; Rohling and Pälike, 2005), which is also evident in climate model simulations (Bauer et al., 2004; Morrill et al., 2013b; Wiersma and Renssen, 2006). Several proxy-based studies have therefore focused on investigating the causal mechanisms, absolute dating, duration, amplitude, spatio-temporal characteristics and environmental consequences of the 8.2 ka event (e.g. Alley and Ágústsdóttir, 2005; Alley et al., 1997; Barber et al., 1999; Boch et al., 2009; Daley et al., 2011; Ellison et al., 2006; Kleiven et al., 2008; Kobashi et al., 2007; Marshall et al., 2007; Morrill and Jacobsen, 2005; Nicolussi and Schlüchter, 2012; Rasmussen et al., 2007; Rohling and Pälike, 2005; Teller et al., 2002; Thomas et al., 2007; Veski et al., 2004; von Grafenstein et al., 1998). However, these studies have so far given only little attention to climate recovery at the demise of the cold event though this could provide important insights into the dynamics and regional peculiarities of rapid climate warming. Likewise, also only very few modelling studies have addressed the resumption of the AMOC and related climatic changes after a freshwater perturbation under Holocene climate boundary conditions in particular (e.g. Renold et al., 2010; Stouffer et al., 2006). Furthermore, the results of climate model simulations for the 8.2 ka event are still ambiguous with respect to the strength and duration of the AMOC slowdown and the following temperature decrease, mostly not matching the proxy evidence (Morrill et al., 2013b). The limitations of climate models in correctly reproducing the full spatio-temporal pattern of climatic changes around 8.2 ka BP are supposedly related to a suite of different factors, involving the complexity and resolution of the models, the probably non-linear response of the AMOC to freshwater forcing (LeGrande and Schmidt, 2008) and a number of not yet well-constrained in-/external forcings (Morrill et al., 2013b), including the volume and rate of freshwater discharge and its exact routing in the North Atlantic (Li et al., 2009; Morrill et al., 2014; Wiersma et al., 2006), the possible role of freshwater background forcing from the melting Laurentide Ice Sheet (Matero et al., 2017; Wagner et al., 2013), the ocean circulation mode around 8.2 ka BP (Born and Levermann, 2010; Morrill et al., 2013b) and the early Holocene climate background state (LeGrande et al., 2006). Hence, there still remain many uncertainties regarding the amplitude and pattern of the AMOC slowdown during the 8.2 ka event and its subsequent recovery as well as regarding the associated climatic changes.

Using analyses of the oxygen isotope ($\delta^{18}\text{O}$) composition of benthic ostracod valves ($\delta^{18}\text{O}_{\text{ostracods}}$) preserved in the varved lake sediments of pre-Alpine Mondsee (Austria), the current study presents a new sub-decadally resolved and precisely dated $\delta^{18}\text{O}$ record from Central Europe for the interval between 7.7 and 8.7 ka BP, providing new information about climate development around 8.2 ka BP. Besides using the detailed characterization of the well-reflected 8.2 ka event in the Mondsee $\delta^{18}\text{O}_{\text{ostracods}}$ record to discuss the suitability of the archive for reconstructing past changes in the oxygen isotope composition of precipitation ($\delta^{18}\text{O}_{\text{precip}}$) and mean annual air temperature (MAAT), we especially focus on climate development at the end of the 8.2 ka event and during the first decades thereafter, an issue so far not sufficiently addressed by proxy-based palaeoclimate studies. In particular, we discuss a previously not described short-term $\delta^{18}\text{O}$ overshoot immediately after the 8.2 ka event, which might reflect a pronounced warming above the pre-8.2 ka event level in Central Europe. Although so far not explicitly interpreted in terms of higher-than-average air temperatures, a similar pattern is also observed in other stable isotope records from the North Atlantic realm, suggesting a signal of hemispheric-scale relevance. By discussing the potential trigger of this episode of possibly higher-than-average air temperatures,

we contribute to a more comprehensive view on climate recovery at the end of the 8.2 ka event. This helps to improve our understanding of the dynamics and mechanisms of rapid climate warming but also challenges climate model simulations.

2. Study site

Mondsee (47°48'N, 13°24'E, 481 m a.s.l.) is a relatively large and deep hardwater lake (lake surface area ~13.8 km², maximum water depth 68 m, lake volume ~0.5 km³, catchment area ~247 km²; Beiwil and Mühlmann, 2008), located ~30 km east of Salzburg (Austria) at the foothills of the Northern Calcareous Alps (Fig. 1). The present-day lake basin established at the end of the last glaciation after the retreat of the Traun Glacier from the area, which most likely occurred already prior to ca. 18,000–19,000 cal years BP (Reitner, 2007; van Husen, 1977, 1997). The lake is at present mainly monomictic with a long stratification period between late April and December and mixing during winter/early spring; dimictic conditions with a short winter stagnation of a few weeks occur only sporadically during the rare years with ice cover (Dokulil and Skolaut, 1986; Ficker et al., 2017; Kämpf et al., 2015). Mondsee is fed by three major tributaries (Fuschler Ache, Zeller Ache, Wangauer Ache), which account for ~70% of the total inflow, as well as several minor creeks. In addition, rainfall on the lake surface and possibly also groundwater flow contribute to the water budget. Lake drainage takes place through a single outlet (Seeache), which has an average discharge of 9.2 m³ s⁻¹, resulting in a theoretical lake water renewal time of ~1.7 years (Jagsch and Megay, 1982; Klee and Schmidt, 1987). The present-day local climate is temperate with a MAAT of 8.5 °C and January and July air temperature means of -1.3 °C and 18.3 °C, respectively. The average annual precipitation sum is 1566 mm with about 50% falling as rain between May and September (all climate data for the period 1981–2010; Central Institute for Meteorology and Geodynamics (ZAMG), Vienna, Austria). Precipitation mainly originates from North Atlantic and Central European sources whereas the Mediterranean contribution north of the Alpine main ridge is at present only minor (~10–17%) (Kaiser et al., 2002; Sodemann and Zubler, 2010). This is corroborated by present-day (1981–2010) wind field data, revealing a dominance of westerly and northwesterly directions with an only minor and seasonally stable contribution from southerly directions (Central Institute for Meteorology and Geodynamics (ZAMG), Vienna, Austria).

3. Material and methods

3.1. Previous work

3.1.1. Lake sediment coring

Two parallel sediment cores (Mo_05_01 and Mo_05_02), each consisting of consecutive 2-m-long core segments, were recovered from a coring site at ~62 m water depth in the southern part of the Mondsee lake basin (47°48'25"N, 13°24'05"E) in June 2005 by using a 90 mm diameter UWITEC piston corer (Lauterbach et al., 2011). Additionally, several short surface sediment cores were recovered with a UWITEC gravity corer from the same location to obtain the undisturbed sediment-water interface. All core segments were subsequently opened, lithostratigraphically described, photographed and subsampled. The overlapping segments of the two piston cores Mo_05_01 and Mo_05_02 and gravity core Mo_05_P3 were visually correlated via distinct macroscopic lithological marker layers, resulting in a continuous composite sediment core of 1493 cm length, which covers more than the last 15 ka, i.e. the complete Holocene and Lateglacial (Lauterbach et al., 2011).

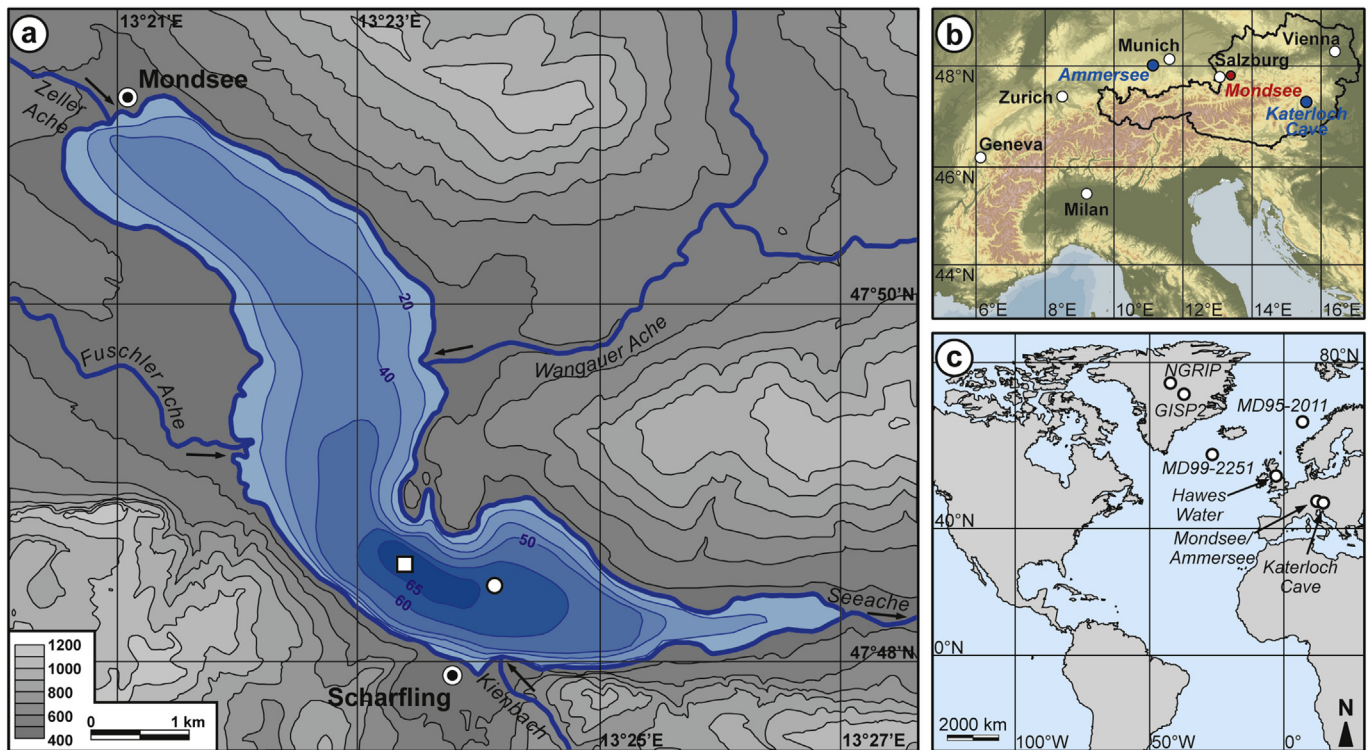


Fig. 1. (a) Schematic bathymetric map of Mondsee (isobaths: water depth in m) and relief of the surrounding area (elevation in m a.s.l.). The coring location at ~62 m water depth is indicated by a white point, the location of the 2011–2013 lake water monitoring for stable isotope analyses is indicated by a white square. (b) Simplified map of the European Alps with the location of Mondsee, Ammersee and Katerloch Cave. (c) Overview map with the location of Mondsee and other proxy records displayed in Fig. 6. (For interpretation of the references to colour in this figure legend, the reader is referred to the web version of this article.)

3.1.2. Chronology of the Holocene Mondsee sediment record

The age model for the Holocene part of the 2005 Mondsee composite sediment core (0–1129 cm composite core depth), whose sediments are composed of biochemical calcite varves with frequently intercalated detrital flood layers (Lauterbach et al., 2011; Swierczynski et al., 2012, 2013a, 2013b), was established through microscopic varve counting on large-scale petrographic thin sections (Lauterbach et al., 2011). This included continuous varve counting in the distinctly laminated upper part of the composite sediment core (0–~610 cm composite core depth), whereas a varve-based sedimentation rate chronology was established for the lower part of the Holocene sediment succession (~610–1129 cm composite core depth) because varve preservation in this interval was often not sufficient to allow continuous counting with reasonable error estimates over larger intervals. Therefore, varve counting and thickness measurements were performed only on well-varved sections here (~15% of the total composite sediment core length between ~610 and 1129 cm) and the resulting average sedimentation rates were transferred to neighbouring intervals with poor varve preservation (cf. electronic supplement to Lauterbach et al., 2011). The reliability of the chronology resulting from this combination of continuous varve counting in the upper part and varve-based sedimentation rate estimates in the lower part is supported by ^{137}Cs dating of the most recent sediments and a set of 28 accelerator mass spectrometry (AMS) ^{14}C dates obtained from terrestrial plant macrofossils, which are evenly distributed across the Holocene sediment sequence (cf. electronic supplement to Lauterbach et al., 2011). A measure of uncertainty for the Holocene Mondsee varve chronology (cf. electronic supplement to Lauterbach et al., 2011) is provided by a comparison of the primary varve count for the uppermost ~610 cm of the 2005 Mondsee composite sediment core with a second independent varve count

that was carried out by a different examiner. For the ca. 4200 years included in this interval, a maximum difference of 50–60 years between both counts (on average < 25 years) was determined, yielding a maximum counting error of 1.25% (Swierczynski et al., 2013b).

3.2. New analyses

3.2.1. Chronology and sedimentological-geochemical analyses

The present study focuses on the interval between 896.0 and 969.0 cm composite core depth of the 2005 Mondsee composite sediment core. The age model for this interval is provided by the published Holocene Mondsee varve chronology (cf. chapter 3.1.2 and electronic supplement to Lauterbach et al., 2011), according to which it covers the time span between ca. 7.7 and 8.7 ka BP, i.e. in a broader sense the interval encompassing the 8.2 ka event. All ages are reported in varve years BP, i.e. before AD 1950. The varve chronology for the early to mid-Holocene part of the 2005 Mondsee composite sediment core, i.e. between ca. 6000 and 10,000 varve years BP (Fig. 2), is supported by a suite of 10 AMS ^{14}C dates (Supplementary Table 3; two additional AMS ^{14}C dates were considered as outliers due to reworking of the dated material or displacement during coring), that are published in the electronic supplement to Lauterbach et al. (2011) and were re-calibrated for the present study using OxCal 4.3 (Bronk Ramsey, 2009) and the IntCal13 calibration data set (Reimer et al., 2013).

To characterize the composition of the Mondsee sediments across the 8.2 ka event and investigate possible sedimentological changes associated with climatic fluctuations, micro X-ray fluorescence (μXRF) element scanning was conducted. Measurements were carried out at the GFZ Potsdam on impregnated sediment slabs from thin section preparation (cf. Lauterbach et al., 2011)

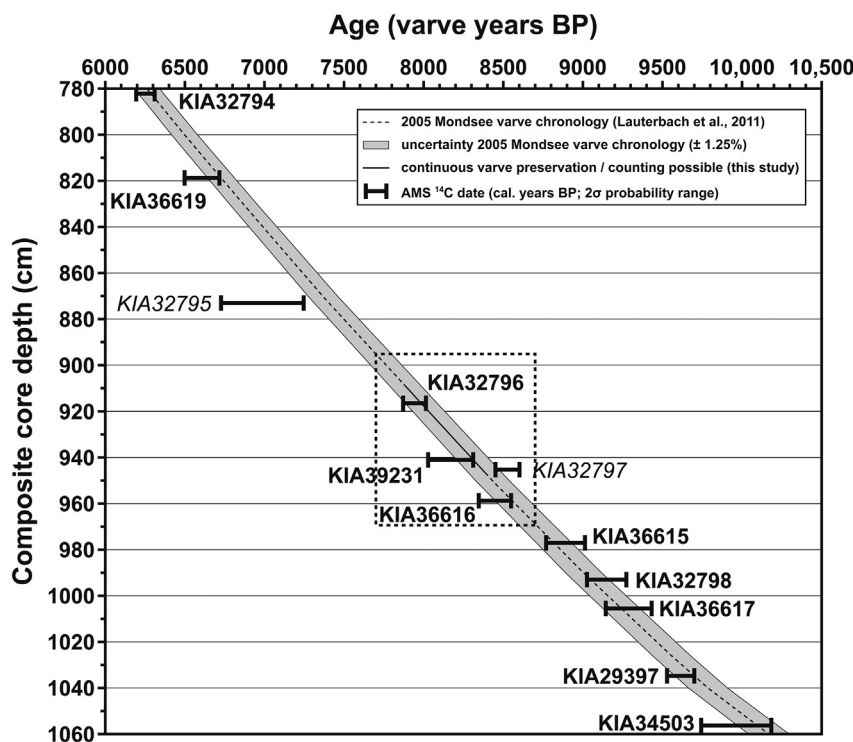


Fig. 2. Age model of the 2005 Mondsee composite sediment core for the interval between 780.0 and 1060.0 cm composite core depth (ca. 6000–10,000 varve years BP) adopted from [Lauterbach et al. \(2011\)](#). The interval investigated within the present study (896.0–969.0 cm) is indicated by a dashed frame, the section with continuously good varve preservation (chapter 4.3) is indicated by a solid line. Calibrated AMS ¹⁴C dates of terrestrial plant macrofossils ([Supplementary Table 3](#)) are given as 2 σ probability ranges. Italicized AMS ¹⁴C dates are considered as outliers, e.g. due to reworking of the dated material or displacement during coring.

between 917.9 and 943.5 cm composite core depth by using a vacuum-operating Eagle III XL μ XRF spectrometer equipped with a Rh X-ray tube operating at 40 kV and 300 mA. Scanning was conducted on a single scan line with a resolution of 200 μ m (250 μ m spot size, 60 s counting time). As intensities of single elements (expressed as counts per second) obtained by μ XRF scanning are influenced by variable sediment properties (e.g. grain size, porosity, content of organic matter and elements not detectable by the μ XRF scanner) and thus non-linearly correlated to element concentrations, the μ XRF scanning results are reported here as log-ratios of selected major elements ($\log(\text{Ca}/\text{Ti})$ and $\log(\text{Ca}/\text{Mg})$) to avoid this possible bias (cf. [Weltje and Tjallingii, 2008](#)).

In addition to μ XRF element scanning, detailed sediment microfacies analysis and varve counting were carried out between 909.0 and 947.0 cm composite core depth by examining the large-scale petrographic thin sections under a Zeiss Axiophot polarisation microscope at 25–400 \times magnification (cf. [Lauterbach et al., 2011](#)).

3.2.2. $\delta^{18}\text{O}$ analyses on ostracod valves

To obtain ostracod valves for $\delta^{18}\text{O}$ analyses for the present study, 0.5-cm-thick slices of bulk sediment (average temporal resolution ~7 years) were taken consecutively from the core segments covering the interval under investigation. The bulk sediment material was subsequently disaggregated in 10% H_2O_2 , followed by wet sieving through a 125 μ m mesh. Retained ostracod valves were rinsed in ethanol and air dried ([von Grafenstein et al., 1998](#)) and juvenile specimens (instars A-2 through A-4) of the species *Candona neglecta* were selected from each subsample. This species has been chosen because (I) it is the most abundant one in the Mondsee sediments ([Namiotko et al., 2015](#)), providing a sufficient number of valves per subsample to establish a continuous $\delta^{18}\text{O}_{\text{Ostracods}}$ record with a high temporal resolution and (II) the isotopic offset for the

non-equilibrium fractionation of valve carbonate of the genus *Candona* compared to calcite precipitated in isotopic equilibrium with the lake water is well-known ([von Grafenstein et al., 1999b](#)).

The oxygen isotope composition of subsets of 13–15 juvenile *Candona neglecta* valves (30–100 μ g total sample weight) picked from each sediment subsample was subsequently analysed at the Leibniz Laboratory for Radiometric Dating and Stable Isotope Research in Kiel. A Finnigan MAT 251 isotope ratio mass spectrometer (IRMS) coupled to a Kiel I preparation device, evolving CO_2 from the valve carbonate by reaction with 100% H_3PO_4 at 75 $^\circ\text{C}$, was used for the analyses. The resulting $\delta^{18}\text{O}_{\text{Ostracods}}$ values ([Supplementary Table 1](#)) are reported relative to the Vienna PeeDee Belemnite (VPDB) standard; the analytical uncertainty is $\pm 0.07\text{‰}$ based on daily routine measurements of different laboratory-internal carbonate standards and the international carbonate standard NBS-19.

3.2.3. Stable isotope analyses of recent water samples

To investigate the link between the oxygen isotope composition of the recent Mondsee lake water ($\delta^{18}\text{O}_{\text{lake}}$) and local $\delta^{18}\text{O}_{\text{precip}}$ and thus to assess the hydrological sensitivity of the lake, water samples from the main tributaries, the outflow and the lake's bottom water were taken in 2005 and 2006. Furthermore, lake water samples integrating over the uppermost 20 m of the water column were collected continuously between December 2011 and October 2013. These samples were analysed for their stable oxygen ($\delta^{18}\text{O}$) and hydrogen (δD) isotope composition at the Alfred Wegener Institute (AWI) in Potsdam and at the Laboratoire des Sciences du Climat et de l'Environnement (LSCE) in Gif-sur-Yvette. At the AWI, samples were processed with a Finnigan MAT Delta-S IRMS, following the gas equilibration technique ([Meyer et al., 2000](#)). Results ([Supplementary Table 2](#)) are given relative to the Vienna Standard

Mean Ocean Water (VSMOW) standard; the analytical precision is $<0.05\text{‰}$ and $<0.5\text{‰}$ for $\delta^{18}\text{O}$ and δD , respectively. At the LSCE, a Finnigan MAT 252 IRMS coupled to a CO_2 -equilibration line and a specially designed mass spectrometer coupled to an automated inlet system were used for $\delta^{18}\text{O}$ and δD measurements, respectively (Vaughn et al., 1998). Results (Supplementary Table 2) are also given relative to the VSMOW standard; the analytical precision is $<0.05\text{‰}$ for $\delta^{18}\text{O}$ and $<1.0\text{‰}$ for δD .

3.2.4. Calculation of $\delta^{18}\text{O}_{\text{lake}}$ from measured $\delta^{18}\text{O}_{\text{ostracods}}$ values

Measured $\delta^{18}\text{O}_{\text{ostracods}}$ (‰ VPDB) values (Supplementary Table 1) were converted into vital-offset-corrected $\delta^{18}\text{O}_{\text{corr.ostracods}}$ (‰ VSMOW) values following equation (1). This included the conversion between the VPDB and VSMOW scales for $\delta^{18}\text{O}$ values of calcite (Friedman and O'Neil, 1977) and a vital offset correction ($\delta^{18}\text{O}_{\text{vital}}$) of $2.2 \pm 0.15\text{‰}$ for the ostracod genus *Candona* (von Grafenstein et al., 1999b), necessary to compensate for the non-equilibrium fractionation of ostracod valve carbonate compared to calcite precipitated in isotopic equilibrium with the lake water.

$$\delta^{18}\text{O}_{\text{corr.ostracods}} (\text{‰ VSMOW}) = 1.03086 \times (\delta^{18}\text{O}_{\text{ostracods}} (\text{‰ VPDB}) - \delta^{18}\text{O}_{\text{vital}}) + 30.86 \quad (1)$$

Past $\delta^{18}\text{O}_{\text{lake}}$ (‰ VSMOW) values (Supplementary Table 1) were then calculated from the $\delta^{18}\text{O}_{\text{corr.ostracods}}$ (‰ VSMOW) values following equations (2) and (3), considering the temperature-dependent fractionation factor ($10^3 \times \ln(\alpha_{\text{calcite-water}})$) between calcite and water (Friedman and O'Neil, 1977) at an average hypolimnetic water temperature (t_{hypo}) of 4.5 °C (Ficker et al., 2017).

$$\delta^{18}\text{O}_{\text{lake}} (\text{‰ VSMOW}) = \delta^{18}\text{O}_{\text{corr.ostracods}} (\text{‰ VSMOW}) - 10^3 \times \ln(\alpha_{\text{calcite-water}}) \quad (2)$$

$$10^3 \times \ln(\alpha_{\text{calcite-water}}) = (2780000 / (t_{\text{hypo}} + 273)^2) - 2.89 \quad (3)$$

Considering the analytical error of the $\delta^{18}\text{O}_{\text{ostracods}}$ measurements ($\pm 0.07\text{‰}$) and the uncertainty of $\delta^{18}\text{O}_{\text{vital}}$ ($\pm 0.15\text{‰}$), the calculated past $\delta^{18}\text{O}_{\text{lake}}$ values have an uncertainty of $\pm 0.17\text{‰}$.

4. Results

4.1. Water stable isotope data and sensitivity of Mondsee to changes in $\delta^{18}\text{O}_{\text{precip}}$

Due to the small ratio between the surface and catchment area of Mondsee and the high average annual precipitation sum in the region (chapter 2), a negligible influence of evaporation effects on the lake water balance can be expected, implying a close link between $\delta^{18}\text{O}_{\text{lake}}$ and local $\delta^{18}\text{O}_{\text{precip}}$. Analyses of the $\delta^{18}\text{O}$ and δD composition of the lake, tributary and outflow water of Mondsee indeed confirm the expected negligible evaporative enrichment of the modern $\delta^{18}\text{O}_{\text{lake}}$ (surface and bottom water) compared to local $\delta^{18}\text{O}_{\text{precip}}$ (Fig. 3), measured at the adjacent monitoring station of

the Austrian Network of Isotopes in Precipitation (ANIP) in Salzburg ($47^\circ 48' \text{N}$, $13^\circ 00' \text{E}$, 430 m a.s.l.). In particular, the present-day lake surface and bottom water reveals a $\delta^{18}\text{O}$ enrichment of $<0.1\text{‰}$ compared to the Local Meteoric Water Line (LMWL) calculated from the Salzburg precipitation $\delta^{18}\text{O}$ and δD data (Fig. 3). Changes of $\delta^{18}\text{O}_{\text{lake}}$ in the upper 20 m of the water column during the monitoring between December 2011 and October 2013 followed the seasonal $\delta^{18}\text{O}_{\text{precip}}$ variations with a temporal delay of ~4 months (highest $\delta^{18}\text{O}_{\text{precip}}$ in summer, highest $\delta^{18}\text{O}_{\text{lake}}$ in autumn) but showed in general only very small seasonal variability with values fluctuating between -9.3 and -10.2‰ , which is $<7\%$ of the range of $\delta^{18}\text{O}_{\text{precip}}$ variability (Fig. 3). Furthermore, $\delta^{18}\text{O}_{\text{lake}}$ in the hypolimnion remains apparently almost constant (only ~1% variability) during the mixing and stagnation period in winter (-10.21‰) and summer (-10.12‰), respectively (Supplementary Table 2). This all indicates an effective buffering of short-term (seasonal) high-amplitude $\delta^{18}\text{O}_{\text{precip}}$ fluctuations (~15‰ in Salzburg; Fig. 3) by the lake system, implying that $\delta^{18}\text{O}_{\text{lake}}$ mainly reflects long-term changes in the average annual $\delta^{18}\text{O}_{\text{precip}}$. Due to the long-term

stability of the hypolimnetic water temperature (Ficker et al., 2017), a significant influence of water temperature variability on the isotopic fractionation between lake water and ostracod valve calcite can also be excluded. In consequence, the $\delta^{18}\text{O}$ composition of ostracod valves from the hypolimnion, which incorporate the isotopic composition of the ambient water during calcification (with a known vital offset due to non-equilibrium fractionation; chapter 3.2.4), can be considered a robust quantitative proxy for

past variations in $\delta^{18}\text{O}_{\text{precip}}$.

4.2. Characteristics and timing of changes in the Mondsee $\delta^{18}\text{O}_{\text{ostracods}}$ record around 8.2 ka BP

In general, the Mondsee $\delta^{18}\text{O}_{\text{ostracods}}$ record between 7.7 and 8.7 ka BP is characterized by high-frequency but only small-scale variability with values fluctuating around a mean of $-5.32 \pm 0.22\text{‰}$ (Fig. 4). However, a distinct 151-year-long interval with $\delta^{18}\text{O}_{\text{ostracods}}$ values of up to $\sim 0.8\text{‰}$ below the 8.7–8.3 ka BP mean of $-5.27 \pm 0.16\text{‰}$ (i.e. the values before the drop) is observed between 8231 and 8080 varve years BP (Fig. 4). This interval of low $\delta^{18}\text{O}_{\text{ostracods}}$ values, which is outstanding as it clearly exceeds 2σ of the general early to mid-Holocene variability (Fig. 5), is interpreted as the 8.2 ka event. It reveals a clear asymmetry with (I) a rapid initial drop in $\delta^{18}\text{O}_{\text{ostracods}}$ by $\sim 0.75\text{‰}$ within 26 years between 8231 and 8205 varve years BP, (II) an 80-year-long central period between 8205 and 8125 varve years BP with $\delta^{18}\text{O}_{\text{ostracods}}$ values $> 0.32\text{‰}$ (2σ) below the 8.7–8.3 ka BP mean and (III) a gradual terminal increase in $\delta^{18}\text{O}_{\text{ostracods}}$ by $\sim 0.5\text{‰}$ within 45 years between 8125 and 8080 varve years BP. The maximum decline in $\delta^{18}\text{O}_{\text{ostracods}}$ ($\sim 1.1\text{‰}$) is observed between 8231 and 8178 varve

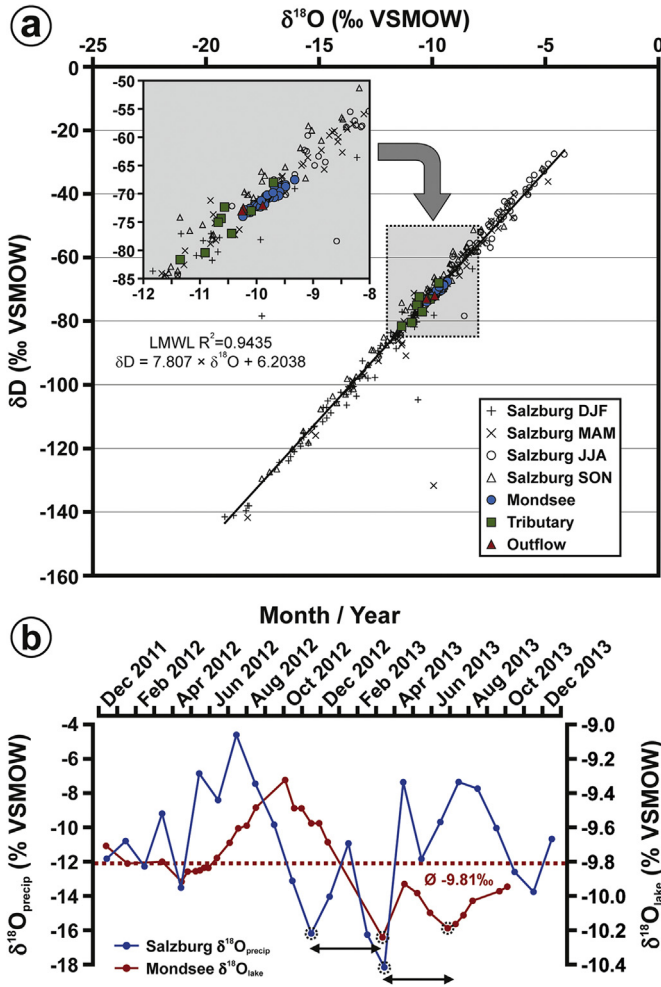


Fig. 3. (a) $\delta^{18}\text{O}$ and δD of recent water samples from Mondsee, its tributaries and its outflow (Supplementary Table 2) as well as local precipitation at the adjacent ANIP monitoring station in Salzburg (1991–2015, seasonal average values) and respective Local Meteoric Water Line (LMWL). (b) $\delta^{18}\text{O}_{\text{lake}}$ of the Mondsee lake surface water (mean of the upper 20 m of the water column) and $\delta^{18}\text{O}_{\text{precip}}$ at the ANIP monitoring station in Salzburg during the monitoring interval 2011–2013. $\delta^{18}\text{O}_{\text{lake}}$ follows $\delta^{18}\text{O}_{\text{precip}}$ but with clearly lower amplitude and a delay of ~4 months between seasonal peaks (arrows between dashed circles). (For interpretation of the references to colour in this figure legend, the reader is referred to the web version of this article.)

years BP. In addition to the clear reflection of the 8.2 ka event, the Mondsee $\delta^{18}\text{O}_{\text{ostracods}}$ record reveals a decadal-scale overshoot in $\delta^{18}\text{O}_{\text{ostracods}}$ directly after the gradual $\delta^{18}\text{O}_{\text{ostracods}}$ rise in the terminal phase of the 8.2 ka event, i.e. between 8080 and 8005 varve years BP. During this short interval, $\delta^{18}\text{O}_{\text{ostracods}}$ values are approximately 0.3–0.4‰ higher than 1σ of the 8.7–8.3 ka BP mean (Fig. 4). After this short period, an immediate decline of $\delta^{18}\text{O}_{\text{ostracods}}$ is observed, reaching again the pre-8.2 ka event level at 7998 varve years BP.

Considering the 1.25% counting error of the Mondsee varve chronology (chapter 3.1.2), the absolute dating uncertainty for the interval around 8.2 ka BP can be estimated to ± 100 years and the error for the duration of the 8.2 ka event itself is ± 2 years. This is confirmed by comparing the primary varve chronology (electronic supplement to Lauterbach et al., 2011) with the result of a new continuous varve count between 935.00 and 923.75 cm composite core depth (i.e. across the interval comprising the isotopically defined 8.2 ka event), that was carried out as a double-check within the present study (Fig. 2). While the duration of this interval is 151

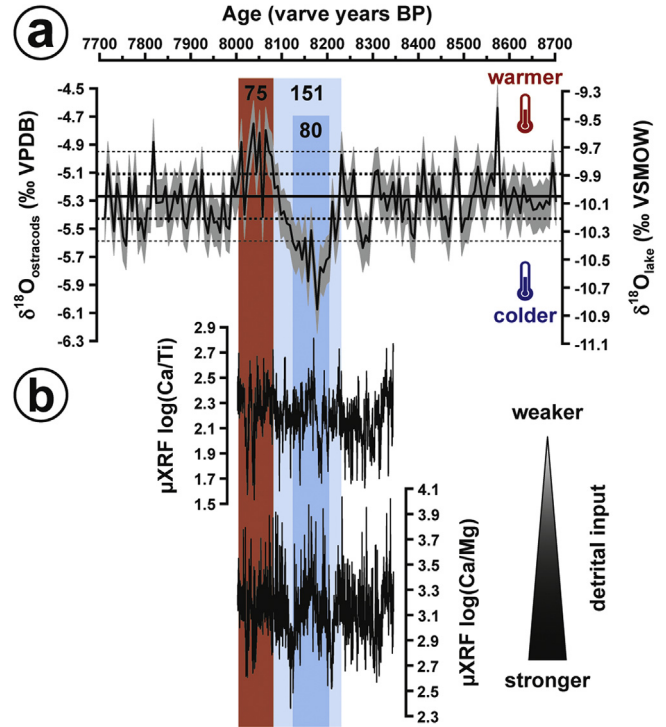


Fig. 4. (a) Measured $\delta^{18}\text{O}_{\text{ostracods}}$ of juvenile *Candona neglecta* valves from the Mondsee sediments and calculated $\delta^{18}\text{O}_{\text{lake}}$ for the interval 7.7–8.7 ka BP (grey shading: absolute error of $\delta^{18}\text{O}_{\text{lake}}$; solid horizontal line: mean of the interval before the 8.2 ka event (8.7–8.3 ka BP); thick dashed lines: $\pm 1\sigma$; thin dashed lines: $\pm 2\sigma$). (b) μXRF scanning log-ratios of selected major elements across the 8.2 ka event, reflecting relative changes in the amount of allochthonous (Ti, Mg) and mainly autochthonous (Ca) sediment components. The light and dark blue bars mark the entire 8.2 ka event and the central period, respectively. The red bar indicates the subsequent $\delta^{18}\text{O}$ overshoot (all durations given in years). (For interpretation of the references to colour in this figure legend, the reader is referred to the web version of this article.)

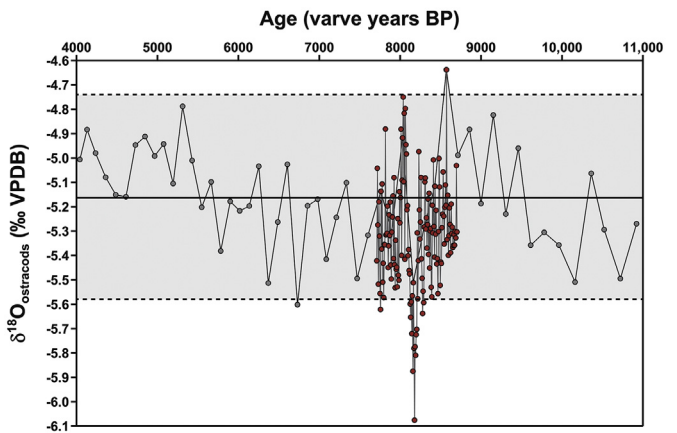


Fig. 5. Comparison of the high-resolution Mondsee $\delta^{18}\text{O}_{\text{ostracods}}$ data obtained across the 8.2 ka event (red dots) with unpublished low-resolution $\delta^{18}\text{O}_{\text{ostracods}}$ data (grey dots, ca. 150–200 years between individual data points) for the interval between 4000 and 11,000 varve years BP. The 2σ of the low-resolution early to mid-Holocene $\delta^{18}\text{O}_{\text{ostracods}}$ data is indicated by the grey shading. (For interpretation of the references to colour in this figure legend, the reader is referred to the web version of this article.)

years according to the primary varve chronology, the floating continuous varve count yielded a duration of 153 years. The difference of 2 years between both approaches confirms the inferred chronological uncertainty of 1.25%, but also indicates that the

primary varve-based sedimentation rate chronology in the lower part of the Mondsee sediment record (below ~610 cm) might slightly underestimate the duration of individual climatic events.

4.3. Sedimentological changes in Mondsee around 8.2 ka BP

Microfacies analysis of the Mondsee sediments reveals no significant changes in general sediment composition across the interval encompassing the isotopically defined 8.2 ka event. The subjective visual evidence is supported by the results of μ XRF element scanning. In particular, the selected element ratios $\log(\text{Ca}/\text{Ti})$ and $\log(\text{Ca}/\text{Mg})$, which semi-quantitatively reflect changes in the relative contribution of allochthonous detrital (Ti, Mg) and mainly autochthonous (Ca) sediment components, show an unchanged high-frequency variability across the 8.2 ka event (Fig. 4), thus indicating the absence of significant changes in precipitation-driven input of detrital material that could correspond to changes in the hydrological regime of the lake. However, despite the lack of obvious changes in sediment composition, varve preservation was found to be generally better for a period of 523 years across the 8.2 ka event, namely between 909.0 and 947.0 cm composite core depth (Fig. 2). This might indicate that the isotopically defined 8.2 ka event is – as proposed by Rohling and Pälike (2005) – superimposed on a centennial-scale period of changed climate conditions that apparently favoured better varve preservation in the Mondsee sediments (e.g. through more pronounced seasonality with a prolonged and more stable stratification period and/or relatively cold winters with lake ice cover, together promoting intensified bottom water anoxia by reducing lake mixing) but were not strong enough to have a more distinct imprint, i.e. to cause changes in sediment composition.

5. Discussion

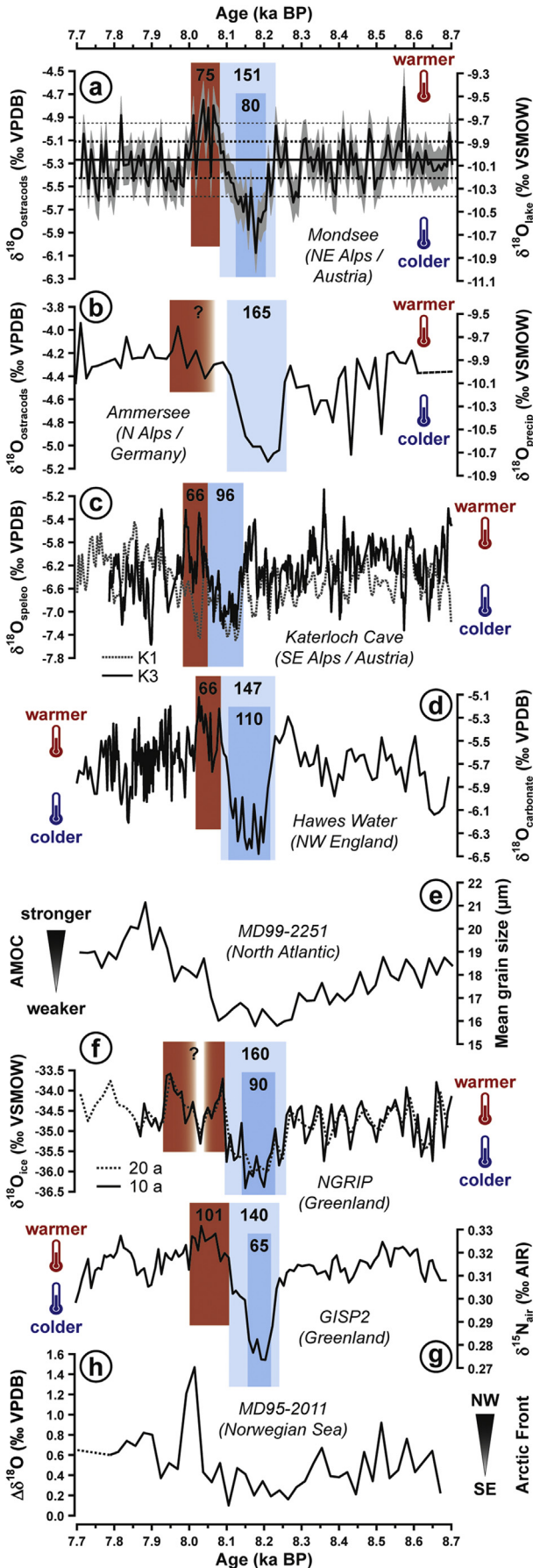
5.1. The 8.2 ka event in the Mondsee $\delta^{18}\text{O}_{\text{ostracods}}$ record and the possible influence of MAAT variability

Although a recent modelling study suggested that the 8.2 ka event might have been caused by centennial-scale meltwater flux from the gradually collapsing Hudson Bay ice saddle (Matero et al., 2017), it is more commonly attributed to the catastrophic drainage of the Laurentide proglacial lakes Agassiz and Ojibway, which supposedly followed the collapse of the Hudson Bay ice dome (Barber et al., 1999; Teller et al., 2002; von Grafenstein et al., 1998; Wiersma and Renssen, 2006) and is dated to ~8470 cal years BP (Barber et al., 1999). The associated sudden discharge of a large amount of freshwater ($1.5\text{--}5.0 \times 10^{14} \text{ m}^3$ or maybe even more within less than a year, equivalent to ~5–10 Sv; $1 \text{ Sv} = 10^6 \text{ m}^3 \text{ s}^{-1}$) via the Hudson Strait into the North Atlantic (Clarke et al., 2004; Teller et al., 2002; Törnqvist et al., 2004; Törnqvist and Hijma, 2012; von Grafenstein et al., 1998; Wiersma et al., 2006) is considered to have caused a salinity/density decrease of the surface waters in the subpolar North Atlantic, which is seen in several proxy records (e.g. Came et al., 2007; Ellison et al., 2006; Thornalley et al., 2009). As a result, the strength of deep convection in the Nordic Seas and consequently also the vigour of southward-flowing deep-water currents in the North Atlantic significantly decreased (Ellison et al., 2006; Kleiven et al., 2008). This is, for example, reflected by a reduction in the strength of the Iceland-Scotland Overflow Water (ISOW), a major contributor to the southward-flowing deep branch of the AMOC (Hansen and Østerhus, 2000), between ca. 8300 and 8100 cal years BP in proxy data from the subpolar North Atlantic (Fig. 6; Ellison et al., 2006). The slowdown of the AMOC caused in turn reduced northward heat transport and consequently a significant decrease of sea surface temperature in

the subpolar North Atlantic (Came et al., 2007; Ellison et al., 2006) as well as air temperature in the North Atlantic realm (Alley and Ágústsdóttir, 2005; Rohling and Pälike, 2005; Wiersma and Renssen, 2006). For example, the cooling at 8.2 ka BP is clearly reflected in a number of precisely dated and quantitatively interpreted stable isotope records from around the North Atlantic, e.g. from the Greenland ice cores (Kobashi et al., 2007; Rasmussen et al., 2007; Thomas et al., 2007), the lacustrine sediment sequences of Ammersee in southern Germany, located ~170 km west of Mondsee (von Grafenstein et al., 1999a; von Grafenstein et al., 1998), and Hawes Water in NW England (Marshall et al., 2007) as well as speleothems from Katerloch Cave in Austria, located ~170 km southeast of Mondsee (Boch et al., 2009). The absolute dating and duration of the 8.2 ka event in all these records is within dating uncertainty (Supplementary Note 1) in good agreement with the marked drop in $\delta^{18}\text{O}_{\text{ostracods}}$ between 8231 and 8080 varve years BP in the Mondsee lake sediment record (Fig. 6 and Table 1), clearly indicating the synchronicity of the event across the North Atlantic realm.

Due to the high hydrological sensitivity of Mondsee, the $\delta^{18}\text{O}_{\text{ostracods}}$ record derived from its sediments can be considered a robust proxy for past changes in $\delta^{18}\text{O}_{\text{precip}}$ (see chapter 4.1). As $\delta^{18}\text{O}_{\text{precip}}$ in Central Europe has been shown to be mainly controlled by air temperature variability in the recent past (Dansgaard, 1964; Rózański et al., 1992; von Grafenstein et al., 1996), the Mondsee $\delta^{18}\text{O}_{\text{ostracods}}$ record can thus be considered in first approximation to reflect past MAAT variability. To roughly assess the amplitude of MAAT changes that could have caused the shifts in the Mondsee $\delta^{18}\text{O}_{\text{ostracods}}$ record during the 8.2 ka event, a present-day $\delta^{18}\text{O}_{\text{precip}}\text{--MAAT}$ gradient of $0.58 \pm 0.11\text{‰ } ^\circ\text{C}^{-1}$, derived from calibrating the Ammersee $\delta^{18}\text{O}_{\text{ostracods}}$ record against a 200-year MAAT record from the nearby meteorological observatory Hohenpeißenberg (von Grafenstein et al., 1996), can be applied to the Mondsee $\delta^{18}\text{O}_{\text{ostracods}}$ data. Since this gradient is fairly similar to that inferred for continental Europe from three decades of continuous monitoring within the framework of GNIP (Rózański et al., 1992) and furthermore holds for a temperature range of ~2 °C, which is approximately the range of Holocene MAAT variability in Central Europe, its application seems reasonable for a first estimate of possible MAAT changes at Mondsee around 8.2 ka BP. Using this gradient, the peak-to-peak amplitude of ~1.1‰ for the drop in the Mondsee $\delta^{18}\text{O}_{\text{ostracods}}$ record between 8231 and 8178 varve years BP would be equivalent to a cooling of ~2.0 °C, which is very similar to the value reported from Ammersee (von Grafenstein et al., 1998). The initial drop in the Mondsee $\delta^{18}\text{O}_{\text{ostracods}}$ record by ~0.75‰ between 8231 and 8205 varve years BP would consequently be equivalent to a cooling of ~1.3 °C, while the central period of the 8.2 ka event between 8205 and 8125 varve years BP would be up to ~1.4 °C colder than the 8.7–8.3 ka BP mean and the terminal ~0.5‰ increase in $\delta^{18}\text{O}_{\text{ostracods}}$ between 8125 and 8080 varve years BP would correspond to a warming of ~0.9 °C. These calculated relative temperature changes can, however, only be regarded as a rough estimate since other possible influences on $\delta^{18}\text{O}_{\text{precip}}$ that are probably superimposed on the predominant control of MAAT variability are not included in this approximation.

First of all, changes in atmospheric circulation (e.g. Teranes and McKenzie, 2001; Yu et al., 1997), leading to shifts in predominant air mass trajectories and the moisture source region (i.e. changes in the relative contribution of Atlantic and Mediterranean air masses), could have influenced the $\delta^{18}\text{O}_{\text{precip}}$ signal. In general, it must be considered that Atlantic air masses reaching the Alps are isotopically more depleted compared to those originating from the Mediterranean because of the longer transport pathway and the more depleted source water (Kaiser et al., 2002). Consequently, a shift towards a higher/lower contribution of isotopically enriched



Mediterranean moisture during the 8.2 ka event, which could occur because of the changed temperature gradients in the North Atlantic realm, would have shifted $\delta^{18}\text{O}_{\text{precip}}$ and thus also the Mondsee $\delta^{18}\text{O}_{\text{ostracods}}$ record to more positive/negative values, thereby biasing a solely temperature-controlled signal. This is supported by modelling data, showing that the European Alps are a quite sensitive region with respect to moisture source changes, i.e. the boundary between more negative North Atlantic and more positive Mediterranean $\delta^{18}\text{O}_{\text{precip}}$ during the 8.2 ka event is shifted northwards in different simulations, causing a positive $\delta^{18}\text{O}_{\text{precip}}$ anomaly at the northern margin of the Alps (LeGrande and Schmidt, 2008). Nevertheless, although an impact of moisture source changes on $\delta^{18}\text{O}_{\text{precip}}$ during the 8.2 ka event can neither be completely excluded nor quantified, it was most likely minor compared to the influence of MAAT variability as the amplitude of the 8.2 ka BP cooling calculated from the Mondsee $\delta^{18}\text{O}_{\text{ostracods}}$ data is very similar (1.5–2.0 °C) to that inferred from pollen-based MAAT reconstructions in the North Atlantic realm (Feurdean et al., 2008; Sarmaja-Korjonen and Seppä, 2007; Veski et al., 2004). Secondly, also changes in the $\delta^{18}\text{O}$ of the ocean water in the dominant moisture source region (i.e. the North Atlantic) caused by the input of the isotopically depleted freshwater could have influenced the Mondsee $\delta^{18}\text{O}_{\text{ostracods}}$ record by lowering $\delta^{18}\text{O}_{\text{precip}}$ without an impact of air temperature changes at the study site. Nevertheless, this scenario most likely also had a rather negligible effect as model simulations have shown that, albeit the freshwater perturbation at 8.2 ka BP caused a large $\delta^{18}\text{O}$ anomaly of the Atlantic surface water, a related significant air temperature-independent lowering of $\delta^{18}\text{O}_{\text{precip}}$ lasted only about two decades in Central Europe with the temperature influence on $\delta^{18}\text{O}_{\text{precip}}$ clearly dominating afterwards (LeGrande and Schmidt, 2008). Finally, also changes in precipitation seasonality (e.g. Drummond et al., 1995), i.e. the relative contribution of isotopically lighter winter precipitation and heavier summer precipitation, could have theoretically influenced the Mondsee $\delta^{18}\text{O}_{\text{ostracods}}$ record in different ways. Possible scenarios would either be a relative increase in the contribution of isotopically heavier summer precipitation (i.e. wetter summers and/or drier winters) or a relative decrease (i.e. drier summers and/or wetter winters). The first scenario would have resulted in more positive $\delta^{18}\text{O}_{\text{precip}}$ values and consequently the temperature decrease during the 8.2 ka event would be underestimated since the effect of more summer precipitation would counteract the $\delta^{18}\text{O}_{\text{precip}}$ decrease arising from reduced MAATs. In contrast, for the second scenario, more negative $\delta^{18}\text{O}_{\text{precip}}$ values should be expected and the temperature decrease during the 8.2 ka event would therefore be overestimated since the relative decrease in the contribution of summer precipitation would shift $\delta^{18}\text{O}_{\text{precip}}$ in the

Fig. 6. Comparison of palaeoclimate records from the North Atlantic realm between ca. 7.7 and 8.7 ka BP (light blue bars: entire 8.2 ka event; dark blue bars: central period; red bars: subsequent stable isotope overshoot; all durations given in years). (a) Mondsee: $\delta^{18}\text{O}_{\text{ostracods}}$ of juvenile *Candona neglecta* valves and calculated $\delta^{18}\text{O}_{\text{lake}}$ (solid horizontal line: 8.7–8.3 ka BP mean; thick dashed lines: $\pm 1\sigma$; thin dashed lines: $\pm 2\sigma$; grey shading: absolute error of the $\delta^{18}\text{O}_{\text{lake}}$ reconstruction). (b) Ammersee: $\delta^{18}\text{O}_{\text{ostracods}}$ of juvenile *Candona* sp. valves and calculated $\delta^{18}\text{O}_{\text{precip}}$ (von Grafenstein et al., 1999a). (c) Katerloch Cave: $\delta^{18}\text{O}_{\text{speleo}}$ of stalagmites K1 and K3 (Boch et al., 2009). (d) Hawes Water: $\delta^{18}\text{O}_{\text{carbonate}}$ of endogenic calcite (original chronology shifted by –200 years; see Supplementary Note 1) (Marshall et al., 2007). (e) Marine core MD99-2251: mean grain size of sortable silt, reflecting changes in ISOW strength/AMOC intensity (Ellison et al., 2006). (f) NGRIP: $\delta^{18}\text{O}_{\text{ice}}$, reflecting air temperature changes (Rasmussen et al., 2007; Thomas et al., 2007). (g) GISP2: $\delta^{15}\text{N}_{\text{air}}$, reflecting air temperature changes (Kobashi et al., 2007). Original data have been transferred to the GICC05 time scale (Seierstad et al., 2014). (h) Marine core MD95-2011: Difference between the $\delta^{18}\text{O}$ of the left- and right-coiling forms of *Neogloboquadrina pachyderma* ($\Delta\delta^{18}\text{O}$), reflecting migration of the Arctic Front (Risebrobakken et al., 2003). (For interpretation of the references to colour in this figure legend, the reader is referred to the web version of this article.)

Table 1
Duration of the entire 8.2 ka event and the central period in different stable isotope records from the North Atlantic realm.

Site	Type of record/measured proxy	Dating method	8.2 ka event (years BP)	Central period (years BP)
Mondsee N Austria	lake sediment/ostracod $\delta^{18}\text{O}$	varve counting ^a	8231–8080	8205–8125
GRIP/NGRIP/DYE-3 Central Greenland (Rasmussen et al., 2007; Thomas et al., 2007)	ice cores/ $\delta^{18}\text{O}_{\text{ice}}$	layer counting ^b (GICC05)	8250–8090	8212–8141
GISP2 Central Greenland (Kobashi et al., 2007; Seierstad et al., 2014)	ice core/ $\delta^{15}\text{N}_{\text{air}}$	layer counting ^b (adjusted to GICC05)	8245–8105	not specified ^d
Ammersee S Germany (von Grafenstein et al., 1999a; von Grafenstein et al., 1998)	lake sediment/ ostracod $\delta^{18}\text{O}$	AMS ¹⁴ C dating	8265–8100	not specified
Katerloch Cave SE Austria (Boch et al., 2009)	speleothems/ carbonate $\delta^{18}\text{O}$	U/Th dating ^b	8196–7962	8146–8050
Hawes Water NW England (Marshall et al., 2007)	lake sediment/ bulk carbonate $\delta^{18}\text{O}$	U/Th dating ^b	8230–8083 ^c	8215–8105 ^c

^a Electronic supplement to Lauterbach et al. (2011).

^b Initial b2k ages converted to years BP (before AD 1950).

^c Original chronology shifted by –200 years.

^d Duration 60–70 years.

same direction as a MAAT reduction. None of these two scenarios can *a priori* be excluded or proven because robust quantitative precipitation reconstructions on a seasonal base for the time interval around 8.2 ka BP are still lacking for the European Alps (Morrill et al., 2013a). However, there is indication from proxy data and model simulations for a coincidence of cool phases and increased summer precipitation in Central Europe during the last 400 years (Wegmann et al., 2014), which, if transferred into the past, would support an underestimation of the temperature changes inferred from the Mondsee $\delta^{18}\text{O}_{\text{ostracods}}$ record. Nevertheless, an important argument against a significant influence of local precipitation seasonality changes on the Mondsee $\delta^{18}\text{O}_{\text{ostracods}}$ record is again the above-mentioned striking similarity of the amplitude of the calculated MAAT drop (~1.5–2.0 °C) with independent, pollen-based MAAT reconstructions (Feurdean et al., 2008; Sarmaja-Korjonen and Seppä, 2007; Veski et al., 2004). Furthermore, also uncertainties regarding the $\delta^{18}\text{O}_{\text{precip}}$ –MAAT relationship in the past hamper a definitive absolute MAAT reconstruction from the Mondsee $\delta^{18}\text{O}_{\text{ostracods}}$ record. In particular, modelling studies provided evidence for a possibly smaller and furthermore non-stationary $\delta^{18}\text{O}_{\text{precip}}$ –MAAT gradient during the 8.2 ka event (~0.4‰ °C⁻¹; LeGrande et al., 2006). If this would be correct, the peak drop of –1.1‰ in the Mondsee $\delta^{18}\text{O}_{\text{ostracods}}$ record during the 8.2 ka event would correspond to a cooling of even ~2.7 °C relative to the 8.7–8.3 ka BP mean, which on the one hand would roughly match the cooling inferred from the Katerloch Cave stalagmites (Boch et al., 2009), but on the other clearly underlines the existing uncertainties in calculating absolute temperature changes around 8.2 ka BP from $\delta^{18}\text{O}$ data without knowing all possible constraints of the $\delta^{18}\text{O}_{\text{precip}}$ –MAAT relationship.

In consequence, it appears that other factors than MAAT variability might have influenced $\delta^{18}\text{O}_{\text{precip}}$ around 8.2 ka BP to a certain but not yet quantifiable degree, inhibiting an absolute quantitative MAAT reconstruction from the Mondsee $\delta^{18}\text{O}_{\text{ostracods}}$ data. However, we are confident that the impact of these factors on $\delta^{18}\text{O}_{\text{precip}}$ was most probably of minor importance, particularly because of the good agreement of our inferred relative temperature changes with independent, pollen-based temperature reconstructions, and therefore consider the Mondsee $\delta^{18}\text{O}_{\text{ostracods}}$ record to reflect in first approximation mainly past MAAT variability.

5.2. Hemispheric-scale evidence for higher-than-average MAATs after the 8.2 ka event

Assuming MAAT variability as the predominant control of the Mondsee $\delta^{18}\text{O}_{\text{ostracods}}$ record and adopting a present-day $\delta^{18}\text{O}_{\text{precip}}$ –MAAT gradient of 0.58 ± 0.11‰ °C⁻¹ (von Grafenstein et al., 1996), the decadal-scale $\delta^{18}\text{O}_{\text{ostracods}}$ overshoot by ~0.3–0.4‰ directly after the 8.2 ka event (Fig. 4) would be equivalent to MAATs approximately 0.5–0.6 °C above the pre-8.2 ka event level. This must, however, be considered as a conservative approximation because of the other possible, not yet quantifiable influences on $\delta^{18}\text{O}_{\text{precip}}$ and the uncertainties regarding the past $\delta^{18}\text{O}_{\text{precip}}$ –MAAT gradient (see chapter 5.1).

Interestingly, a period of higher-than-average MAATs directly after the 8.2 ka event that would be similar to our interpretation of the Mondsee $\delta^{18}\text{O}_{\text{ostracods}}$ data has never been particularly emphasized elsewhere although numerous proxy records from the North Atlantic realm provide unequivocal evidence for the 8.2 ka BP cooling. Nevertheless, a detailed re-evaluation of published regional palaeoclimate records shows that a similar signal after the 8.2 ka event is visible in several other stable isotope records as well, even if it has not been explicitly interpreted in terms of higher-than-average air temperatures. For example, elevated $\delta^{18}\text{O}$ values of endogenic calcite after the 8.2 ka event can be observed in lake sediment records from western Ireland (Holmes et al., 2016) and Hawes Water (Marshall et al., 2007) and also the ostracod-based $\delta^{18}\text{O}$ record from Ammersee (von Grafenstein et al., 1999a; von Grafenstein et al., 1998) reveals slightly elevated $\delta^{18}\text{O}$ values after the 8.2 ka event (Fig. 6), although the signal is less clearly expressed here. However, the weaker signal in the Ammersee $\delta^{18}\text{O}_{\text{ostracods}}$ record can be easily explained by archive sensitivity and analytical resolution. On the one hand, the lower hydrological sensitivity (water renewal time ~2.7 years for Ammersee vs. ~1.7 years for Mondsee) could have subdued the high-amplitude $\delta^{18}\text{O}$ fluctuations seen in the Mondsee record after the 8.2 ka event by integrating high-frequency $\delta^{18}\text{O}_{\text{precip}}$ variability over a longer time interval, thus balancing out extreme values. On the other hand, the lower temporal resolution of the Ammersee data set (~15–25 years) might also have a suppressing effect by integrating the probably existing sub-decadal variability in the $\delta^{18}\text{O}_{\text{ostracods}}$ data – as visible in the Mondsee record – over a period of up to two

decades.

Further indication for overshooting $\delta^{18}\text{O}$ values after the 8.2 ka event in the Alps comes from a stalagmite (K3) from Katerloch Cave (Fig. 6; Boch et al., 2009). However, the evidence is not as unambiguous as in Mondsee since a second stalagmite (K1) from this cave does not show a similarly well-expressed signal. A possible explanation for the differences between the two individual stalagmites could be a relatively strong influence of site-specific factors (e.g. changes in cave hydrology), probably overprinting the regional/hemispheric-scale climate signal to a certain degree. This idea is supported by the generally higher amplitude of $\delta^{18}\text{O}$ changes (including the more pronounced high-frequency variability) and the more complex structure of the 8.2 ka event (apparently two-phased in stalagmite K1) compared to the lake sediment records (Fig. 6). On the other hand, the discrepancies between the Mondsee and Katerloch Cave $\delta^{18}\text{O}$ records could also be related to the different relative contribution of Atlantic and Mediterranean moisture sources and the isotopic contrast between both. While Mondsee at the northern flank of the Alps is mainly influenced by Atlantic air masses, Katerloch Cave at the southern Alpine rim is more influenced by the Mediterranean (Sodemann and Zubler, 2010). Isotopic observations and the calculation of backward trajectories have shown that during summer, i.e. the high-precipitation season in the Alpine realm, even a large change in the relative contribution of Mediterranean moisture to precipitation south of the Alpine main ridge (from 19% to 36%) would be accompanied by only a relatively minor shift (from 10% to 14%) north of it (Kaiser et al., 2002). Due to the larger influence of Mediterranean moisture south of the Alps, it could therefore be that the Katerloch Cave stalagmites recorded to some extent a Mediterranean climate signal. As Holocene $\delta^{18}\text{O}$ records from the Mediterranean region have been shown to reflect in many cases not only temperature variability but also changes in regional hydroclimate (e.g. Dean et al., 2015; Frisia et al., 2006), this could also explain the more ambiguous evidence for a post-8.2 ka event $\delta^{18}\text{O}$ overshoot in the Katerloch Cave stalagmites.

In addition to the indication from European palaeoclimate records, further evidence for possibly increased air temperatures after the 8.2 ka event is provided by stable isotope records from the Greenland ice cores. In particular, overshooting isotope values after the 8.2 ka event are observed at 8095–8060 years BP in the NGRIP $\delta^{18}\text{O}_{\text{ice}}$ and at 8105–8005 years BP in the GISP2 $\delta^{15}\text{N}_{\text{air}}$ record (Fig. 6; Kobashi et al., 2007; Rasmussen et al., 2007; Seierstad et al., 2014; Thomas et al., 2007), of which particularly the latter is considered to robustly reflect past air temperature variability. Although the isotope overshoots in the Greenland ice core records after the 8.2 ka event have not been explicitly discussed in terms of increased air temperatures so far, the signals show a remarkable similarity and synchronicity with the Mondsee $\delta^{18}\text{O}_{\text{ostracods}}$ record. In conclusion, based on the fact that a similar isotope overshoot after the 8.2 ka event as that observed in the Mondsee $\delta^{18}\text{O}_{\text{ostracods}}$ record is also evident in several other stable isotope records from the North Atlantic realm (Fig. 6), we infer that this phenomenon is of hemispheric-scale rather than local significance.

5.3. A possible trigger mechanism for pronounced warming after the 8.2 ka event

An explanation for the possible occurrence of higher-than-average MAATs directly after the 8.2 ka event as inferred from the Mondsee $\delta^{18}\text{O}_{\text{ostracods}}$ record could be a pronounced recovery of the AMOC. This hypothesis is supported by proxy data from the subpolar North Atlantic, showing an increase in the ISOW near-bottom flow speed at about 8100 cal years BP (Fig. 6; Ellison et al., 2006), i.e. ca. 200–400 years after the initial freshwater perturbation (Barber

et al., 1999). This strengthening of the ISOW flow speed can be considered as a robust indication for the onset of a pronounced AMOC recovery, being in good agreement with some model experiments, which also revealed an enhanced resumption of the AMOC ca. 200–400 years after the end of a freshwater perturbation (Renold et al., 2010; Stouffer et al., 2006). Although the AMOC response to freshwater forcing in general and particularly the occurrence of an enhanced AMOC resumption after a freshwater perturbation strongly depends on model setup and sensitivity as well as the input parameters (Morrill et al., 2013b), some modelling studies have proposed reasonable trigger mechanisms for such an enhanced AMOC resumption. On the one hand, it could be related to northward salt transport by the subtropical gyre, causing the recovery of salinity in the high latitudes (Vellinga et al., 2002). On the other hand, it could also be caused by the release of heat accumulated in the deep Atlantic Ocean during the AMOC slowdown (Renssen et al., 2007). In particular, it has been postulated that the ocean water density gradient and thus the limited meridional ocean water exchange would be gradually reduced by advective processes after cessation of the freshwater input, slowly strengthening the AMOC until crossing a certain density threshold in the subpolar North Atlantic (Renold et al., 2010). Subsequently, abrupt local convection should commence, leading to an AMOC intensification by ~60% within a few decades (Renold et al., 2010). According to coupled ocean-atmosphere climate models, the AMOC intensification should then cause enhanced heat transport, i.e. the advance of warm, highly saline water, into the high northern latitudes, a result nicely corresponding to proxy evidence from the Norwegian Sea, showing a NW migration of the Arctic Front around 8000 cal years BP (Fig. 6; Risebrobakken et al., 2003). Furthermore, the reinforced heat transport should be responsible for a positive MAAT anomaly in the North Atlantic realm (Renssen et al., 2007; Wiersma and Renssen, 2006; Wiersma et al., 2011). In particular, model simulations indicate a MAAT anomaly of ~0.5 °C above the pre-8.2 ka event level for the area north of 45°N (Renssen et al., 2007), occurring ca. 200–300 years after the initial freshwater perturbation (Wiersma et al., 2011). This is in good agreement with our estimates from the Mondsee $\delta^{18}\text{O}_{\text{ostracods}}$ record when considering MAAT as the primary control of $\delta^{18}\text{O}_{\text{precip}}$ variability.

6. Conclusions

The varve-dated Mondsee $\delta^{18}\text{O}_{\text{ostracods}}$ record provides proxy evidence for a $\delta^{18}\text{O}_{\text{precip}}$ overshoot in Central Europe during the first decades after the 8.2 ka event (i.e. between 8080 and 8005 varve years BP), which was likely caused by an enhanced AMOC recovery and possibly reflects an interval of higher-than-average MAATs. Enhanced AMOC recovery after the 8.2 ka event has previously been suggested by climate model simulations and indication for a similar climate signal, i.e. more positive stable isotope values that possibly reflect increased MAATs, can be found in several high- and mid-latitude proxy records from the North Atlantic realm. While this possible temperature anomaly might not be detectable in many palaeoclimate records due to proxy/archive insensitivity, local threshold effects and/or insufficient temporal resolution, it has apparently been overlooked or at least not been explicitly described in several others so far, challenging the future interpretation of proxy records. Even if the interpretation of $\delta^{18}\text{O}$ records in terms of absolute temperature changes in the past still needs to be further constrained, especially by robust precipitation reconstructions, the Mondsee $\delta^{18}\text{O}_{\text{ostracods}}$ record for the interval around 8.2 ka BP can be regarded a valuable contribution to a better understanding of the dynamics of rapid Holocene climatic changes and their underlying trigger mechanisms. Furthermore, it provides important information for testing the performance of climate model

simulations. Nevertheless, additional high-resolution investigations are required to verify the regional significance of climatic changes around 8.2 ka BP.

Author contributions

N.A., S.L., A.B., U.v.G and H.E. conceived the study and jointly interpreted the proxy data; S.L. led the writing of the manuscript with contributions to discussion and writing from A.B., N.A., H.E. and U.v.G.; U.v.G., A.B., H.E., D.L.D., M.H. and S.B. participated in the coring campaign; S.L. was responsible for the establishment of the varve chronology; M.H. and H.E. provided radiocarbon dates; P.D. carried out the μ XRF measurements; D.L.D., T.N., S.B. and U.v.G. were responsible for ostracod sampling and taxonomy and N.A. performed the $\delta^{18}\text{O}$ measurements on the ostracod valves; C.N., S.B. and U.v.G. were responsible for water isotope sampling and U.v.G., S.B., C.N., H.M. and B.C. performed the water isotope analyses.

Acknowledgements

This study was funded as a part of the ESF EuroCLIMATE project Declakes (project 04-ECLIM-FP29) through grants from the FWF (I35-B06), DFG (AN 554/1-2, BR 2208/2-2) and CNRS. We thank G. Roidmayr, M. Pichler, D. Berger, G. Arnold, M. Köhler, R. Niederreiter, Á. Baltanás, M. Desmet, B. Fanget, J. Nomade and J. Knoll for field and lab assistance and L. Kämpf for running the 2011–2013 lake water monitoring. The Institute for Water Ecology, Fisheries and Lake Research in Scharfling (particularly A. Jagsch and G. Bruschek) and the Research Institute for Limnology of the University of Innsbruck in Mondsee (particularly H. Höllner) are acknowledged for logistic support. We thank Ana Moreno for editorial handling as well as C. Spötl and two anonymous reviewers for comments that helped to improve the manuscript. This is a contribution to the Helmholtz Association climate initiative REKLIM (Topic 8 – Rapid climate change from proxy data) and COST Action ES0907 INTIMATE. The Mondsee $\delta^{18}\text{O}_{\text{ostracods}}$ and calculated $\delta^{18}\text{O}_{\text{lake}}$ values are available in [Supplementary Table 1](#) and via the PANGAEA database (<https://www.pangaea.de>).

Appendix A. Supplementary data

Supplementary data related to this article can be found at <http://dx.doi.org/10.1016/j.quascirev.2017.08.001>.

References

- Alley, R.B., Ágústsson, A.M., 2005. The 8k event: cause and consequences of a major Holocene abrupt climate change. *Quat. Sci. Rev.* 24, 1123–1149. <https://doi.org/10.1016/j.quascirev.2004.12.004>.
- Alley, R.B., Mayewski, P.A., Sowers, T., Stuiver, M., Taylor, K.C., Clark, P.U., 1997. Holocene climatic instability: a prominent, widespread event 8200 yr ago. *Geology* 25, 483–486. [https://doi.org/10.1130/0091-7613\(1997\)025<0483:HCIAPW>2.3.CO;2](https://doi.org/10.1130/0091-7613(1997)025<0483:HCIAPW>2.3.CO;2).
- Barber, D.C., Dyke, A., Hillaire-Marcel, C., Jennings, A.E., Andrews, J.T., Kerwin, M.W., Bilodeau, G., McNeely, R., Southon, J., Morehead, M.D., Gagnon, J.M., 1999. Forcing of the cold event of 8,200 years ago by catastrophic drainage of Laurentide lakes. *Nature* 400, 344–348. <https://doi.org/10.1038/22504>.
- Bauer, E., Ganopolski, A., Montoya, M., 2004. Simulation of the cold climate event 8200 years ago by meltwater outburst from Lake Agassiz. *Paleoceanography* 19, PA3014. <https://doi.org/10.1029/2004pa001030>.
- Beiw, C., Mühlmann, H., 2008. Atlas der natürlichen Seen Österreichs mit einer Fläche ≥ 50 ha. Morphometrie – Typisierung – Trophie. Bundesamt für Wasserwirtschaft, Vienna.
- Boch, R., Spötl, C., Kramers, J., 2009. High-resolution isotope records of early Holocene rapid climate change from two coeval stalagmites of Katerloch Cave, Austria. *Quat. Sci. Rev.* 28, 2527–2538. <https://doi.org/10.1016/j.quascirev.2009.05.015>.
- Born, A., Levermann, A., 2010. The 8.2 ka event: abrupt transition of the subpolar gyre toward a modern North Atlantic circulation. *Geochim. Geophys. Geosys.* 11, Q06011. <https://doi.org/10.1029/2009GC003024>.
- Bronk Ramsey, C., 2009. Bayesian analysis of radiocarbon dates. *Radiocarbon* 51, 337–360. <https://doi.org/10.1017/S0033822200033865>.
- Came, R.E., Oppo, D.W., McManus, J.F., 2007. Amplitude and timing of temperature and salinity variability in the subpolar North Atlantic over the past 10 ky. *Geology* 35, 315–318. <https://doi.org/10.1130/g23455a.1>.
- Clarke, G.K.C., Leverington, D.W., Teller, J.T., Dyke, A.S., 2004. Paleohydraulics of the last outburst flood from glacial Lake Agassiz and the 8200 BP cold event. *Quat. Sci. Rev.* 23, 389–407. <https://doi.org/10.1016/j.quascirev.2003.06.004>.
- Daley, T.J., Thomas, E.R., Holmes, J.A., Street-Perrott, F.A., Chapman, M.R., Tindall, J.C., Valdes, P.J., Loader, N.J., Marshall, J.D., Wolff, E.W., Hopley, P.J., Atkinson, T., Barber, K.E., Fisher, E.H., Robertson, I., Hughes, P.D.M., Roberts, C.N., 2011. The 8200 a yr BP cold event in stable isotope records from the North Atlantic region. *Glob. Planet. Change* 79, 288–302. <https://doi.org/10.1016/j.gloplacha.2011.03.006>.
- Dansgaard, W., 1964. Stable isotopes in precipitation. *Tellus* 16, 436–468. <https://doi.org/10.1111/j.2153-3490.1964.tb00181.x>.
- Dean, J.R., Jones, M.D., Leng, M.J., Noble, S.R., Metcalfe, S.E., Sloane, H.J., Sahy, D., Eastwood, W.J., Roberts, C.N., 2015. Eastern Mediterranean hydroclimate over the late glacial and Holocene, reconstructed from the sediments of Nar lake, central Turkey, using stable isotopes and carbonate mineralogy. *Quat. Sci. Rev.* 124, 162–174. <https://doi.org/10.1016/j.quascirev.2015.07.023>.
- Dokulil, M., Skolaut, C., 1986. Succession of phytoplankton in a deep stratifying lake: Mondsee, Austria. *Hydrobiologia* 138, 9–24. <https://doi.org/10.1007/BF00027229>.
- Drummond, C.N., Patterson, W.P., Walker, J.C.G., 1995. Climatic forcing of carbon-oxygen isotopic covariance in temperate-region marl lakes. *Geology* 23, 1031–1034. [https://doi.org/10.1130/0091-7613\(1995\)023<1031:CFOCO>2.3.CO;2](https://doi.org/10.1130/0091-7613(1995)023<1031:CFOCO>2.3.CO;2).
- Ellison, C.R.W., Chapman, M.R., Hall, I.R., 2006. Surface and deep ocean interactions during the cold climate event 8200 years ago. *Science* 312, 1929–1932. <https://doi.org/10.1126/science.1127213>.
- Feurdean, A., Klotz, S., Mosbrugger, V., Wohlfarth, B., 2008. Pollen-based quantitative reconstructions of Holocene climate variability in NW Romania. *Palaeogeogr. Palaeoclimatol. Palaeoecol.* 260, 494–504. <https://doi.org/10.1016/j.palaeo.2007.12.014>.
- Ficker, H., Luger, M., Gassner, H., 2017. From dimictic to monomictic: empirical evidence of thermal regime transitions in three deep alpine lakes in Austria induced by climate change. *Freshw. Biol.* 62, 1335–1345. <https://doi.org/10.1111/fwb.12946>.
- Friedman, I., O'Neil, J.R., 1977. Compilation of stable isotope fractionation factors of geochemical interest. In: Fleischer, M. (Ed.), *Data of Geochemistry*, sixth ed., p. 115 USGS Professional Paper 440-KK.
- Frisia, S., Borsato, A., Mangini, A., Spötl, C., Madonia, G., Sauro, U., 2006. Holocene climate variability in Sicily from a discontinuous stalagmite record and the Mesolithic to Neolithic transition. *Quat. Res.* 66, 388–400. <https://doi.org/10.1016/j.yqres.2006.05.003>.
- Hansen, B., Østerhus, S., 2000. North Atlantic–Nordic seas exchanges. *Prog. Oceanogr.* 45, 109–208. [https://doi.org/10.1016/S0079-6611\(99\)00052-X](https://doi.org/10.1016/S0079-6611(99)00052-X).
- Holmes, J.A., Tindall, J., Roberts, N., Marshall, W., Marshall, J.D., Bingham, A., Feeser, I., O'Connell, M., Atkinson, T., Jourdan, A.-L., March, A., Fisher, E.H., 2016. Lake isotope records of the 8200-year cooling event in western Ireland: comparison with model simulations. *Quat. Sci. Rev.* 131, 341–349. <https://doi.org/10.1016/j.quascirev.2015.06.027>.
- Jagsch, A., Megay, K., 1982. Mondsee. In: Wurzer, E. (Ed.), *Seenreinigung in Österreich*. Bundesministerium für Land- und Forstwirtschaft, Wien, Wasserwirtschaft 6, pp. 155–163.
- Kaiser, A., Scheifinger, H., Kralik, M., Papesch, W., Rank, D., Stöckl, W., 2002. Links between meteorological conditions and spatial/temporal variations in long-term isotope records from the Austrian precipitation network. In: International Atomic Energy Agency (Ed.), *Study of Environmental Change Using Isotope Techniques*. C&S Paper Series 13/P, Vienna, Austria, pp. 66–76.
- Kämpf, L., Mueller, P., Höllner, H., Plessen, B., Naumann, R., Thoss, H., Güntner, A., Merz, B., Brauer, A., 2015. Hydrological and sedimentological processes of flood layer formation in Lake Mondsee. *Depositional Rec.* 1, 18–37. <https://doi.org/10.1002/dep2.2>.
- Klee, R., Schmidt, R., 1987. Eutrophication of Mondsee (Upper Austria) as indicated by the diatom stratigraphy of a sediment core. *Diatom. Res.* 2, 55–76. <https://doi.org/10.1080/0269249X.1987.9704985>.
- Kleiven, H.F., Kissel, C., Laj, C., Ninnemann, U.S., Richter, T.O., Cortijo, E., 2008. Reduced North Atlantic deep water coeval with the Glacial Lake Agassiz freshwater outburst. *Science* 319, 60–64. <https://doi.org/10.1126/science.1148924>.
- Kobashi, T., Severinghaus, J.P., Brook, E.J., Barnola, J.M., Grachev, A.M., 2007. Precise timing and characterization of abrupt climate change 8200 years ago from air trapped in polar ice. *Quat. Sci. Rev.* 26, 1212–1222. <https://doi.org/10.1016/j.quascirev.2007.01.009>.
- Lauterbach, S., Brauer, A., Andersen, N., Danielopol, D.L., Dulski, P., Hüls, M., Milecka, K., Namiotko, T., Obrenska, M., von Grafenstein, U., Declakes participants, 2011. Environmental responses to Lateglacial climatic fluctuations recorded in the sediments of pre-Alpine Lake Mondsee (northeastern Alps). *J. Quat. Sci.* 26, 253–267. <https://doi.org/10.1002/jqs.1448>.
- LeGrande, A.N., Schmidt, G.A., 2008. Ensemble, water isotope-enabled, coupled general circulation modeling insights into the 8.2 ka event. *Paleoceanography* 23, PA3207. <https://doi.org/10.1029/2008PA001610>.
- LeGrande, A.N., Schmidt, G.A., Shindell, D.T., Field, C.V., Miller, R.L., Koch, D.M.,

- Faluvegi, G., Hoffmann, G., 2006. Consistent simulations of multiple proxy responses to an abrupt climate change event. *Proc. Natl. Acad. Sci. U. S. A.* 103, 837–842. <https://doi.org/10.1073/pnas.0510095103>.
- Li, Y.X., Renssen, H., Wiersma, A.P., Törnqvist, T.E., 2009. Investigating the impact of Lake Agassiz drainage routes on the 8.2 ka cold event with a climate model. *Clim. Past* 5, 471–480. <https://doi.org/10.5194/cp-5-471-2009>.
- Marshall, J.D., Lang, B., Crowley, S.F., Weedon, G.P., van Calsteren, P., Fisher, E.H., Holme, R., Holmes, J.A., Jones, R.T., Bedford, A., Brooks, S.J., Bloemendal, J., Kiriakoulakis, K., Ball, J.D., 2007. Terrestrial impact of abrupt changes in the North Atlantic thermohaline circulation: early Holocene, UK. *Geology* 35, 639–642. <https://doi.org/10.1130/G23498A.1>.
- Matero, I.S.O., Gregoire, L.J., Ivanovic, R.F., Tindall, J.C., Haywood, A.M., 2017. The 8.2 ka cooling event caused by Laurentide ice saddle collapse. *Earth Planet. Sci. Lett.* 473, 205–214. <https://doi.org/10.1016/j.epsl.2017.06.011>.
- Mayewski, P.A., Rohling, E.E., Stager, C.J., Karlen, W., Maasch, K.A., Meeker, L.D., Meyerson, E.A., Gasse, F., van Kreveld, S., Holmgren, K., Lee-Thorp, J., Rosqvist, G., Rack, F., Staubwasser, M., Schneider, R.R., Steig, E.J., 2004. Holocene climate variability. *Quat. Res.* 62, 243–255. <https://doi.org/10.1016/j.yqres.2004.07.001>.
- Meyer, H., Schönicke, L., Wand, U., Hubberten, H.W., Friedrichsen, H., 2000. Isotope studies of hydrogen and oxygen in ground ice – experiences with the equilibration technique. *Isotopes Environ. Health Stud.* 36, 133–149. <https://doi.org/10.1080/10256010008032939>.
- Morrill, C., Anderson, D.M., Bauer, B.A., Buckner, R., Gille, E.P., Gross, W.S., Hartman, M., Shah, A., 2013a. Proxy benchmarks for intercomparison of 8.2 ka simulations. *Clim. Past* 9, 423–432. <https://doi.org/10.5194/cp-9-423-2013>.
- Morrill, C., Jacobsen, R.M., 2005. How widespread were climate anomalies 8200 years ago? *Geophys. Res. Lett.* 32, L19701. <https://doi.org/10.1029/2005GL023536>.
- Morrill, C., LeGrande, A.N., Renssen, H., Bakker, P., Otto-Bliesner, B.L., 2013b. Model sensitivity to North Atlantic freshwater forcing at 8.2 ka. *Clim. Past* 9, 955–968. <https://doi.org/10.5194/cp-9-955-2013>.
- Morrill, C., Ward, E.M., Wagner, A.J., Otto-Bliesner, B.L., Rosenbloom, N., 2014. Large sensitivity to freshwater forcing location in 8.2 ka simulations. *Paleoceanography* 29, 930–945. <https://doi.org/10.1002/2014pa002669>.
- Namiotko, T., Danielopol, D.L., von Grafenstein, U., Lauterbach, S., Brauer, A., Andersen, N., Hüls, M., Milecka, K., Baltanás, A., Geiger, W., DecLakes Participants, 2015. Palaeoecology of Late Glacial and Holocene profundal Ostracoda of pre-Alpine lake Mondsee (Austria) – a base for further (palaeo-)biological research. *Palaeogeogr. Palaeoclimatol. Palaeoecol.* 419, 23–36. <https://doi.org/10.1016/j.palaeo.2014.09.009>.
- Nicolussi, K., Schlüchter, C., 2012. The 8.2 ka event – calendar-dated glacier response in the Alps. *Geology* 40, 819–822. <https://doi.org/10.1130/G32406.1>.
- Rasmussen, S.O., Vinther, B.M., Clausen, H.B., Andersen, K.K., 2007. Early Holocene climate oscillations recorded in three Greenland ice cores. *Quat. Sci. Rev.* 26, 1907–1914. <https://doi.org/10.1016/j.quascirev.2007.06.015>.
- Reimer, P.J., Bard, E., Bayliss, A., Beck, J.W., Blackwell, P.G., Bronk Ramsey, C., Buck, C.E., Cheng, H., Edwards, R.L., Friedrich, M., Grootes, P.M., Guilderson, T.P., Haffidason, H., Hajdas, I., Hatté, C., Heaton, T.J., Hoffmann, D.L., Hogg, A.G., Hughen, K.A., Kaiser, K.F., Kromer, B., Manning, S.W., Niu, M., Reimer, R.W., Richards, D.A., Scott, E.M., Southon, J.R., Staff, R.A., Turney, C.S.M., van der Plicht, J., 2013. IntCal13 and Marine13 radiocarbon age calibration curves 0–50,000 Years cal BP. *Radiocarbon* 55, 1869–1887. https://doi.org/10.2458/azu_js_rc.55.16947.
- Reitner, J.M., 2007. Glacial dynamics at the beginning of Termination I in the Eastern Alps and their stratigraphic implications. *Quat. Int.* 164–65, 64–84. <https://doi.org/10.1016/j.quaint.2006.12.016>.
- Renold, M., Raible, C.C., Yoshimori, M., Stocker, T.F., 2010. Simulated resumption of the North Atlantic meridional overturning circulation – slow basin-wide advection and abrupt local convection. *Quat. Sci. Rev.* 29, 101–112. <https://doi.org/10.1016/j.quascirev.2009.11.005>.
- Renssen, H., Goosse, H., Fichefet, T., 2007. Simulation of Holocene cooling events in a coupled climate model. *Quat. Sci. Rev.* 26, 2019–2029. <https://doi.org/10.1016/j.quascirev.2007.07.011>.
- Risebrobakken, B., Jansen, E., Andersson, C., Mjelde, E., Hevrøy, K., 2003. A high-resolution study of Holocene paleoclimatic and paleoceanographic changes in the Nordic Seas. *Paleoceanography* 18 (1017). <https://doi.org/10.1029/2002PA000764>.
- Rohling, E.J., Pälike, H., 2005. Centennial-scale climate cooling with a sudden cold event around 8,200 years ago. *Nature* 434, 975–979. <https://doi.org/10.1038/nature03421>.
- Różański, K., Araguas-Araguas, L., Gonfiantini, R., 1992. Relation between long-term trends of oxygen-18 isotope composition of precipitation and climate. *Science* 258, 981–985. <https://doi.org/10.1126/science.258.5084.981>.
- Sarmaja-Korjonen, K., Seppä, H., 2007. Abrupt and consistent responses of aquatic and terrestrial ecosystems to the 8200 cal. yr cold event; a lacustrine record from Lake Arapisto, Finland. *Holocene* 17, 457–467. <https://doi.org/10.1177/0959683607077020>.
- Seierstad, I.K., Abbott, P.M., Bigler, M., Blunier, T., Bourne, A.J., Brook, E., Buchardt, S.L., Buizert, C., Clausen, H.B., Cook, E., Dahl-Jensen, D., Davies, S.M., Guillevic, M., Johnsen, S.J., Pedersen, D.S., Popp, T.J., Rasmussen, S.O., Severinghaus, J.P., Svensson, A., Vinther, B.M., 2014. Consistently dated records from the Greenland GRIP, GISP2 and NGRIP ice cores for the past 104 ka reveal regional millennial-scale $\delta^{18}\text{O}$ gradients with possible Heinrich event imprint. *Quat. Sci. Rev.* 106, 29–46. <https://doi.org/10.1016/j.quascirev.2014.10.032>.
- Sodemann, H., Zubler, E., 2010. Seasonal and inter-annual variability of the moisture sources for Alpine precipitation during 1995–2002. *Int. J. Climatol.* 30, 947–961. <https://doi.org/10.1002/joc.1932>.
- Stouffer, R.J., Yin, J., Gregory, J.M., Dixon, K.W., Spelman, M.J., Hurlin, W., Weaver, A.J., Eby, M., Flato, G.M., Hasumi, H., Hu, A., Jungclaus, J.H., Kamenkovich, I.V., Levermann, A., Montoya, M., Murakami, S., Nawrath, S., Oka, A., Peltier, W.R., Robitaille, D.Y., Sokolov, A., Vettoretti, G., Weber, S.L., 2006. Investigating the causes of the response of the thermohaline circulation to past and future climate changes. *J. Clim.* 19, 1365–1387. <https://doi.org/10.1175/JCLI3689.1>.
- Swierczynski, T., Brauer, A., Lauterbach, S., Martin-Puertas, C., Dulski, P., von Grafenstein, U., Rohr, C., 2012. A 1600 yr seasonally resolved record of decadal-scale flood variability from the Austrian Pre-Alps. *Geology* 40, 1047–1050. <https://doi.org/10.1130/g33493.1>.
- Swierczynski, T., Lauterbach, S., Dulski, P., Brauer, A., 2013a. Late Neolithic Mondsee Culture in Austria: living on lakes and living with flood risk? *Clim. Past* 9, 1601–1612. <https://doi.org/10.5194/cp-9-1601-2013>.
- Swierczynski, T., Lauterbach, S., Dulski, P., Delgado, J., Merz, B., Brauer, A., 2013b. Mid- to late Holocene flood frequency changes in the northeastern Alps as recorded in varved sediments of Lake Mondsee (Upper Austria). *Quat. Sci. Rev.* 80, 78–90. <https://doi.org/10.1016/j.quascirev.2013.08.018>.
- Teller, J.T., Leverington, D.W., Mann, J.D., 2002. Freshwater outbursts to the oceans from glacial Lake Agassiz and their role in climate change during the last deglaciation. *Quat. Sci. Rev.* 21, 879–887. [https://doi.org/10.1016/S0277-3791\(01\)00145-7](https://doi.org/10.1016/S0277-3791(01)00145-7).
- Teranes, J.L., McKenzie, J.A., 2001. Lacustrine oxygen isotope record of 20th-century climate change in central Europe: evaluation of climatic controls on oxygen isotopes in precipitation. *J. Paleolimnol.* 26, 131–146. <https://doi.org/10.1023/A:1011175701502>.
- Thomas, E.R., Wolff, E.C., Mulvaney, R., Steffensen, J.P., Johnsen, S.J., Arrowsmith, C., White, J.W.C., Vaughn, B., Popp, T., 2007. The 8.2 ka event from Greenland ice cores. *Quat. Sci. Rev.* 26, 70–81. <https://doi.org/10.1016/j.quascirev.2006.07.017>.
- Thornalley, D.J.R., Elderfield, H., McCave, I.N., 2009. Holocene oscillations in temperature and salinity of the surface subpolar North Atlantic. *Nature* 457, 711–714. <https://doi.org/10.1038/nature07717>.
- Törnqvist, T.E., Bick, S.J., González, J.L., van der Borg, K., de Jong, A.F.M., 2004. Tracking the sea-level signature of the 8.2 ka cooling event: new constraints from the Mississippi Delta. *Geophys. Res. Lett.* 31, L23309. <https://doi.org/10.1029/2004GL021429>.
- Törnqvist, T.E., Hijma, M.P., 2012. Links between early Holocene ice-sheet decay, sea-level rise and abrupt climate change. *Nat. Geosci.* 5, 601–606. <https://doi.org/10.1038/ngeo1536>.
- van Husen, D., 1977. Zur Fazies und Stratigraphie der jungpleistozänen Ablagerungen im Trauntal. *Jahrb. Geol. Bundesanst. Wien* 120, 1–130.
- van Husen, D., 1997. LGM and late-glacial fluctuations in the Eastern Alps. *Quat. Int.* 38–39, 109–118. [https://doi.org/10.1016/S1040-6182\(96\)00017-1](https://doi.org/10.1016/S1040-6182(96)00017-1).
- Vaughn, B.H., White, J.W.C., Delmotte, M., Trolier, M., Cattani, O., Stievenard, M., 1998. An automated system for hydrogen isotope analysis of water. *Chem. Geol.* 152, 309–319. [https://doi.org/10.1016/S0009-2541\(98\)00117-X](https://doi.org/10.1016/S0009-2541(98)00117-X).
- Vellinga, M., Wood, R.A., Gregory, J.M., 2002. Processes governing the recovery of a perturbed thermohaline circulation in HadCM3. *J. Clim.* 15, 764–780. [https://doi.org/10.1175/1520-0442\(2002\)015<0764:PGTROA>2.0.CO;2](https://doi.org/10.1175/1520-0442(2002)015<0764:PGTROA>2.0.CO;2).
- Veski, S., Seppä, H., Ojala, A.E.K., 2004. Cold event at 8200 yr BP recorded in annually laminated lake sediments in eastern Europe. *Geology* 32, 681–684. <https://doi.org/10.1130/G20683.1>.
- von Grafenstein, U., Erlenkeuser, H., Brauer, A., Jouzel, J., Johnsen, S.J., 1999a. A mid-European decadal isotope-climate record from 15,500 to 5000 years B.P. *Science* 284, 1654–1657. <https://doi.org/10.1126/science.284.5420.1654>.
- von Grafenstein, U., Erlenkeuser, H., Müller, J., Jouzel, J., Johnsen, S.J., 1998. The cold event 8200 years ago documented in oxygen isotope records of precipitation in Europe and Greenland. *Clim. Dynam.* 14, 73–81. <https://doi.org/10.1007/s003820050210>.
- von Grafenstein, U., Erlenkeuser, H., Müller, J., Trimborn, P., Alefs, J., 1996. A 200 year mid-European air temperature record preserved in lake sediments: an extension of the $\delta^{18}\text{O}_{\text{p}}$ -air temperature relation into the past. *Geochim. Cosmochim. Acta* 60, 4025–4036. [https://doi.org/10.1016/S0016-7037\(96\)00230-X](https://doi.org/10.1016/S0016-7037(96)00230-X).
- von Grafenstein, U., Erlenkeuser, H., Trimborn, P., 1999b. Oxygen and carbon isotopes in modern fresh-water ostracod valves: assessing vital offsets and autecological effects of interest for paleoclimatic studies. *Palaeogeogr. Palaeoclimatol. Palaeoecol.* 148, 133–152. [https://doi.org/10.1016/S0031-0182\(98\)00180-1](https://doi.org/10.1016/S0031-0182(98)00180-1).
- Wagner, A.J., Morrill, C., Otto-Bliesner, B.L., Rosenbloom, N., Watkins, K.R., 2013. Model support for forcing of the 8.2 ka event by meltwater from the Hudson Bay ice dome. *Clim. Dynam.* 41, 2855–2873. <https://doi.org/10.1007/s00382-013-1706-z>.
- Wegmann, M., Brönnimann, S., Bhend, J., Franke, J., Folini, D., Wild, M., Luterbacher, J., 2014. Volcanic influence on European summer precipitation through monsoons: possible cause for “years without summer”. *J. Clim.* 27, 3683–3691. <https://doi.org/10.1175/JCLI-D-13-00524.1>.
- Weltje, G.J., Tjallingii, R., 2008. Calibration of XRF core scanners for quantitative geochemical logging of sediment cores: theory and application. *Earth Planet. Sci. Lett.* 274, 423–438. <https://doi.org/10.1016/j.epsl.2008.07.054>.
- Wiersma, A.P., Renssen, H., 2006. Model-data comparison for the 8.2 ka BP event: confirmation of a forcing mechanism by catastrophic drainage of Laurentide lakes. *Quat. Sci. Rev.* 25, 63–88. <https://doi.org/10.1016/j.quascirev.2005.07.009>.

- Wiersma, A.P., Renssen, H., Goosse, H., Fichefet, T., 2006. Evaluation of different freshwater forcing scenarios for the 8.2 ka BP event in a coupled climate model. *Clim. Dynam.* 27, 831–849. <https://doi.org/10.1007/s00382-006-0166-0>.
- Wiersma, A.P., Roche, D.M., Renssen, H., 2011. Fingerprinting the 8.2 ka event climate response in a coupled climate model. *J. Quat. Sci.* 26, 118–127. <https://doi.org/10.1002/jqs.1439>.
- Yu, Z., McAndrews, J.H., Eicher, U., 1997. Middle Holocene dry climate caused by change in atmospheric circulation patterns: evidence from lake levels and stable isotopes. *Geology* 25, 251–254 [https://doi.org/10.1130/0091-7613\(1997\)025<0251:MHDCCB>2.3.CO;2](https://doi.org/10.1130/0091-7613(1997)025<0251:MHDCCB>2.3.CO;2).